

Phase field simulation for the evolution of textured ceramics microstructure

Liangliang Liu^a, Feng Gao^{a,*}, Guoxin Hu^a, Jiangnan Liu^{a,b}

^a State Key Laboratory of Solidification Processing, College of Material Science and Engineering, Northwestern Polytechnical University, Xi'an 710072, China

^b Xi'an Polytechnic University, Xi'an 710048, China

Received 20 June 2011; received in revised form 6 March 2012; accepted 23 March 2012

Available online 1 April 2012

Abstract

A modified model using phase field method in order to describe grain-oriented growth is developed. The evolution of the long-range order (*lro*) parameter fields is governed by the time-dependent Ginzburg–Landau equation. Periodic boundary conditions are implemented in simulation. The gradient energy coefficient k_i is allowed to depend on both the parameters along x -axis (k_x) and z -axis (k_z). Anisotropic coefficient C is proposed to describe the ratio of k_x to k_z . Interface energy anisotropy causes significant deviation of grain growth kinetics from the one observed in isotropic system and does change the size and shape of grains. When the interface energy is anisotropic, the ratio of the average mean linear intercept (MLI) in the different direction is time-dependent and self-similarity does not hold anymore. The value of anisotropic coefficient C strongly influences grain growth behavior. The simulation result is consistent with the experimental result of textured ceramics prepared by reaction templated grain growth.

© 2012 Elsevier Ltd and Techna Group S.r.l. All rights reserved.

Keywords: A. Grain growth; Phase field simulation; Textured ceramics; Microstructure

1. Introduction

Grain-oriented growth is an interesting and important issue, which controls number of physical and mechanical properties of polycrystalline materials. However, most of the previous theoretical and experimental investigations were concerned with normal grain growth during which the average grain size increases while the shape of the size distribution remains constant [1]. There is increasing evidence that certain properties of a material can be improved by deliberately introducing anisotropic grains in a fine-grain matrix. For example, electrical properties can be improved with anisotropic grains. Textured $(\text{Na}_{0.85}\text{K}_{0.15})_{0.5}\text{Bi}_{0.5}\text{TiO}_3$ ceramics were fabricated by RTGG and tape-casting technique [2]. The textured ceramics have a microstructure with developed plated-like grains aligned in the direction parallel to the tape casting plane. The ceramics show anisotropic dielectric and piezoelectric properties in the directions parallel and perpendicular to the casting plane.

Grain-oriented growth is a very complicated process. Many factors can affect the degree of texture, such as differences in grain boundary energy, the difference in solubility between grains [3], the presence of a liquid phase [4] and the content of anisotropic template particles [5]. Due to the difficulty of directly incorporating topological features into analytical theories of grain growth [6], there has been increasing interest in using computer simulations to study grain growth in single-phase materials. The most frequently used numerical techniques include: finite element method [7], Monte Carlo Potts model [8], cellular automata model [9] and phase-field model [10,11]. There have recently been remarkable advances in the simulations of microstructural evolution by the phase-field models [12]. In the models, the boundary energy is introduced through gradient energy terms in free energy functional. The main advantage of this model is that continuous tracking of grain boundary position is not required since the locations of grain boundaries are implicitly defined by the regions where the gradients of field variables are not zero. Another important feature of the phase-field model is that anisotropy in interface energy can be easily handled [13–15]. Kazaryan and Wang [16] have investigated grain growth in systems of anisotropic grain boundary energy and mobility by phase field method. In their studies, the energy

* Corresponding author. Tel.: +86 13096956133.

E-mail address: gaofeng@nwpu.edu.cn (F. Gao).

and mobility are allowed to depend on both grain boundary inclination and misorientation. In RTGG process [4], the template particles with anisotropic interface energy are aligned with a specific orientation by tape casting, which means that the highest interface energy orientation of template particles is set parallel to the direction along the casting plane. However, the conventional template particle has a rhombohedral or tetragonal crystal structure [2–5]. The interface energy in one direction (z -axis) exhibits a higher value which will result in the different grain growth rate. Therefore, the preferred orientation of grain growth is definite in RTGG process, which can be simulated by simple phase field model. Absolutely, it is not sensible to use their model simulating the RTGG process because it is complicated and time-consuming.

In this paper, a modified phase field model for grain-oriented growth is developed. We focus on texture evolution of grain-oriented growth along a certain direction (x -axis, e.g. casting direction). The theoretical formulation is first presented, followed by numerical simulations in the x - z plane, and a discussion concludes the paper.

2. Phase field model

According to the phase field model for grain growth in single phase materials explained in [17] the following set of non-conserved order parameter fields $\eta_1(r, t)$, $\eta_2(r, t)$, ..., $\eta_p(r, t)$ were used to represent the polycrystalline microstructure, where p is the number of possible orientations a grain in space. In real materials, the number of orientations is infinite, but a finite value of p ($p > 36$) is often sufficient for reasonably accurate simulations of grain growth [17]. The total free energy of the inhomogeneous system can be written

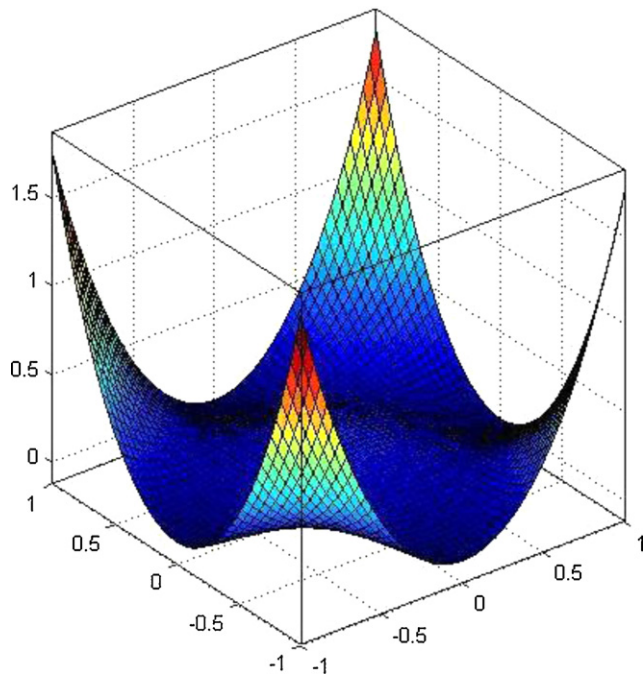


Fig. 1. Free energy density with two orientation variables.

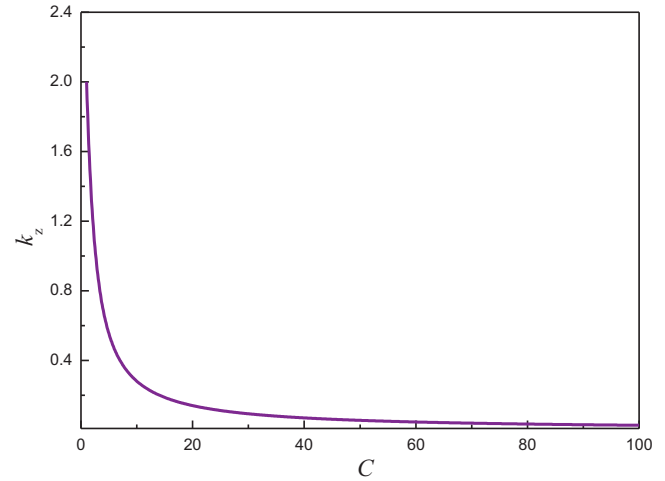


Fig. 2. k_z as a function of C .

as [18]:

$$F = F_0$$

$$+ \int \left[f(\eta_1(r), \eta_2(r), \dots, \eta_p(r)) + \sum_{i=1}^p \frac{k_i}{2} (\nabla \eta_i(r))^2 \right] d^3r. \quad (1)$$

where f is the free energy density as a function of the phase-field variables and k_i is the gradient energy coefficient. Chen and Yang [18] propose the following expression for the free energy density f of a polycrystalline material:

$$f(\eta_1, \eta_2, \dots, \eta_p) = \sum_{i=1}^p \left[-\frac{\alpha}{2} \eta_i^2 + \frac{\beta}{4} \eta_i^4 \right] + \gamma \sum_{i=1}^p \sum_{j>i}^p \eta_i^2 \eta_j^2. \quad (2)$$

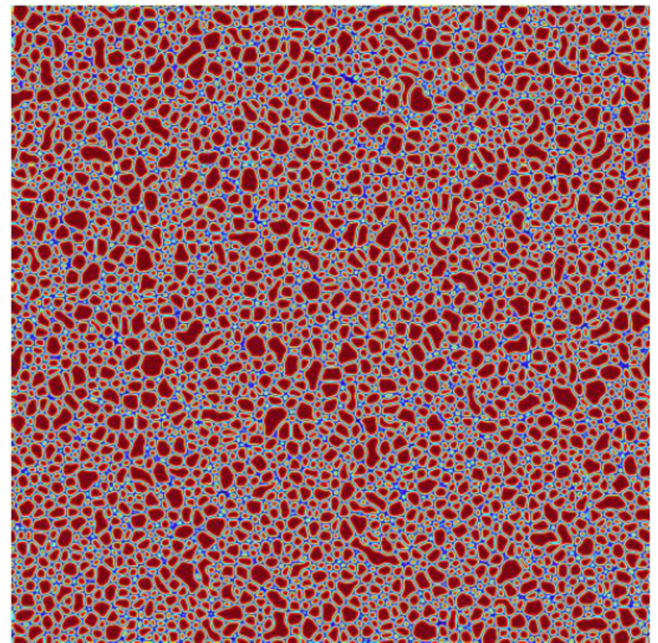


Fig. 3. Initial microstructure, which was used for all simulations. (For interpretation of the references to color in the text, the reader is referred to the web version of this article.)

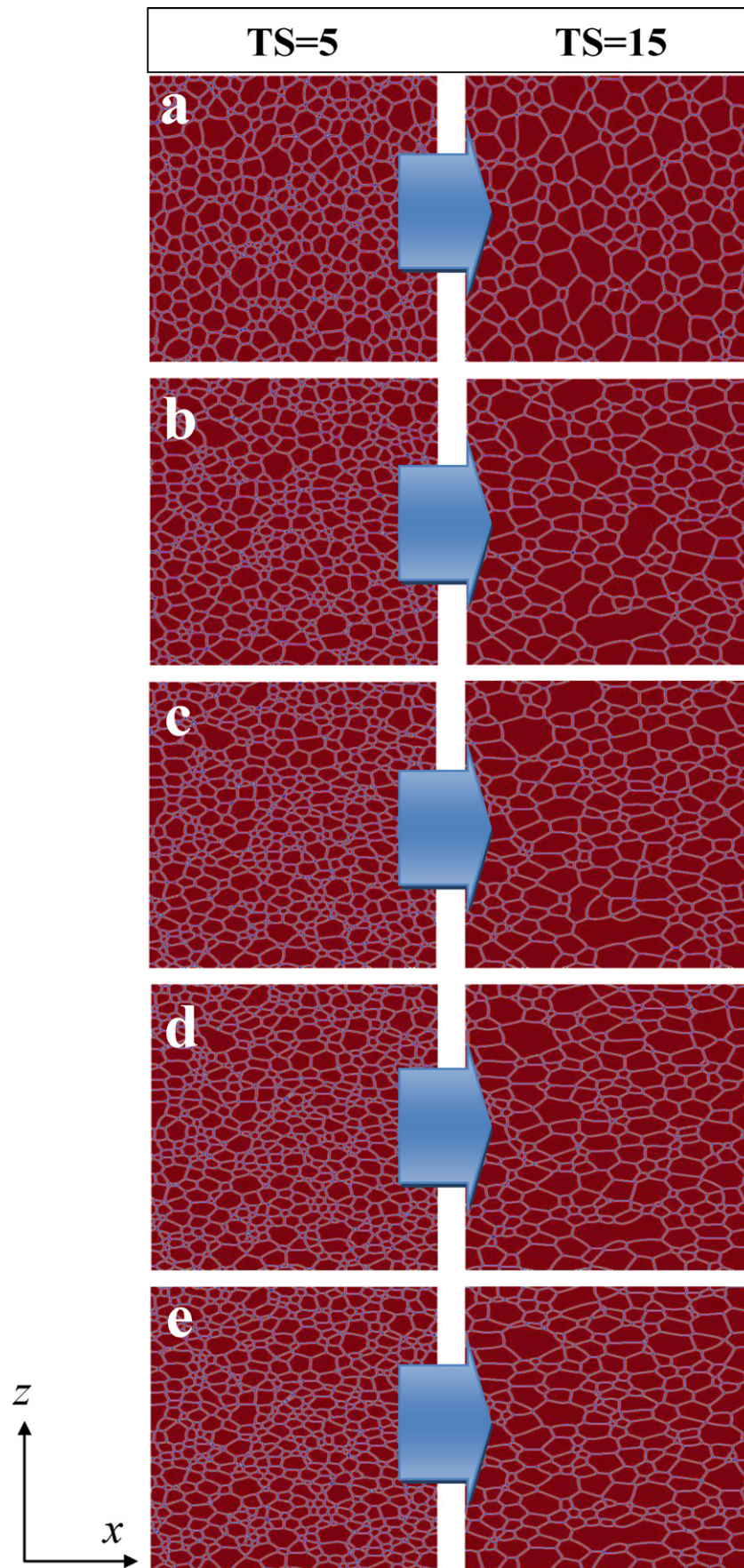


Fig. 4. Topological evolution of grain growth at (a) $C = 1$; (b) $C = 5$; (c) $C = 10$; (d) $C = 20$; (e) $C = 30$.

where α , β and γ are positive constants. The free energy expression has $2p$ degenerate minima with equal depth at $\{\eta_i = \pm 1, \eta_{j \neq i} = 0, i, j = 1, \dots, p\}$ reflecting the p orientations a grain can have. For a particular order parameter η_i , f has minima at $\eta_i = \pm 1$ when all the other order parameters equal zero. An example of the free energy density with $p = 2$, $\alpha = \beta = \gamma = 1.0$ is shown in Fig. 1 in which there are four minima located at $(\eta_1, \eta_2) = (1, 0), (0, 1), (-1, 0)$ and $(0, -1)$.

The time-dependent Ginzburg–Landau equation for the order parameter fields can be expressed as follows:

$$\frac{d\eta_i(r, t)}{dt} = -L_i \frac{\delta F}{\delta \eta_i(r, t)}. \quad (3)$$

where L_i is the mobility of grain boundary migration. Using the expression for f given in (2) and then substituting the total free energy F (Eq. (1)) into Eq. (3), we obtain:

$$\frac{d\eta_i}{dt} = -L_i \left[-\alpha \eta_i + \beta \eta_i^3 + 2\gamma \eta_i \sum_{j \neq i}^p \eta_j - k_i \nabla^2 \eta_i \right]. \quad (4)$$

In our model, the anisotropic template grains were set parallel to the direction along the casting plane. So, the grain has maximum surface energy in the direction of x -axis and minimum surface energy in the perpendicular direction, e.g. z -axis. Thus, we can discrete k_i in the x – z rectangular coordinate system as:

$$k_x = Ck_z. \quad (5)$$

where k_x and k_z are the gradient energy coefficients along x -axis and z -axis and C relates to the crystalline structure. For example, when the value of one phase-field variable at (x_0, z_0) lattice point is calculated, the Laplacian item in Eq. (4) can be decomposed into a set of algebraic equations:

$$k_i \nabla^2 \eta = k_x \frac{\eta_{x_0-1, z_0} + \eta_{x_0+1, z_0} - 2\eta_{x_0, z_0}}{\Delta x^2} + k_z \frac{\eta_{x_0, z_0-1} + \eta_{x_0, z_0+1} - 2\eta_{x_0, z_0}}{\Delta z^2} \quad (6)$$

To simplify the computer program, we define parameter C as a constant, anisotropic coefficient. Periodic boundary conditions are implemented in the course of simulation. We selected the following numerical values for the parameters in the kinetic equations: $\alpha = \beta = \gamma = 1.0$, $k_i = 2.0$, $L = 1.0$, $\Delta t = 0.15$, $\Delta x = 2.0$. In order to examine the effect of the value of C on the microstructure development under invariable total free energy conditions, we set the modulus of the gradient energy coefficients k_i as a constant, as follow:

$$\sqrt{\frac{(k_x^2 + k_z^2)}{2}} = k_i. \quad (7)$$

From relation (5), Eq. (7) can be rearranged as:

$$k_z = \sqrt{\frac{8}{C^2 + 1}}. \quad (8)$$

Fig. 2 shows the relation between k_z and C . It is easy to see that the value of k_z significantly decreased for $C < 10$ and

varied slowly for $C > 20$. When C increases from 1 to 10, the value of k_z decreased by 85.93%. And a decrease of 7.01% was observed in the value of C changing from 10 to 20. In this study, the values of C (1, 5, 10, 20 and 30) were chosen as research examples.

The system size is 512×512 grid points. The simulations are started from a disordered structure with $\eta_i \approx 0$, i.e. at all grid points, small random values between -0.001 and 0.001 are assigned to the order parameters. Then, the order parameter fields are allowed to evolve according to Eq. (4). We set only for the liquid phase because we assumed that our system included no pores. We can take the earlier grain nucleation as template and the left liquid as matrix. Thus, the initial microstructure is generated after $200\Delta t$ as shown in Fig. 3. Here, time scale was measured in terms of time step (TS). TS = 1 means one $1000\Delta t$.

To show the microstructural evolution, we defined the function $\varphi(\mathbf{r})$ as follow:

$$\varphi(\mathbf{r}) = \sum_{i=1}^p \eta_i^2(\mathbf{r}). \quad (9)$$

The value of $\varphi(\mathbf{r})$ was displayed using color image with wine red area representing $\varphi(\mathbf{r}) = 1$ and blue $\varphi(\mathbf{r}) = 0$, e.g. grains are wine red and grain boundaries blue. MATLAB software was used for the visualization of φ .

3. Simulation results and discussion

3.1. Microstructure evolution

Fig. 4 shows simulation results of the grain growth for x – z plane in 2D system. The evolution process of the isotropic grain growth ($C = 1$) is displayed in Fig. 4(a). After 0.3 time steps the grains impinge and a fine grained microstructure is formed. The microstructure evolves in a way determined by the reduction of the excess free energy. It is shown that the smaller grains get absorbed into the larger grains so that the number of grain sides and sizes increase gradually. Due to the isotropy of the grain boundary energy, the grains evolve in a self-similar manner into

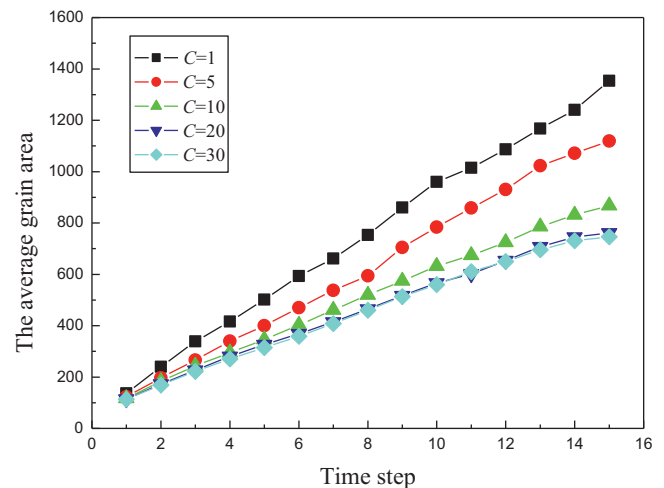


Fig. 5. Change of the average grain area with different C .

equi-axial shapes. Fig. 4(b)–(e) shows the simulation results of grain-oriented growth for $C = 5, 10, 20$ and 30 , respectively. It is readily seen that anisotropic coefficient C significantly change the shapes of grains. In the case of $C = 5$ (Fig. 4(b)) used in the simulations, the shape of some grains become plate-like morphology. With $C = 10, 20$ and 30 employed in this study, there is an increased number of grain boundaries with horizontal direction and almost all grains evolve in plate-like morphology. This is the reason that the directions which move

fast are those with high boundary mobility. When some grains impinge upon each other, one grain has the highest grain boundary mobility at the direction of x -axis and the lowest grain boundary mobility at the direction of z -axis compared to other grains. This grain in high mobility direction tends to grow fast whereas the low mobility direction tends to grow slowly so that it becomes elongated and grows larger. Other grains grow slowly or are consumed by elongated grains during the growth competition. At the low mobility directions, grains can still

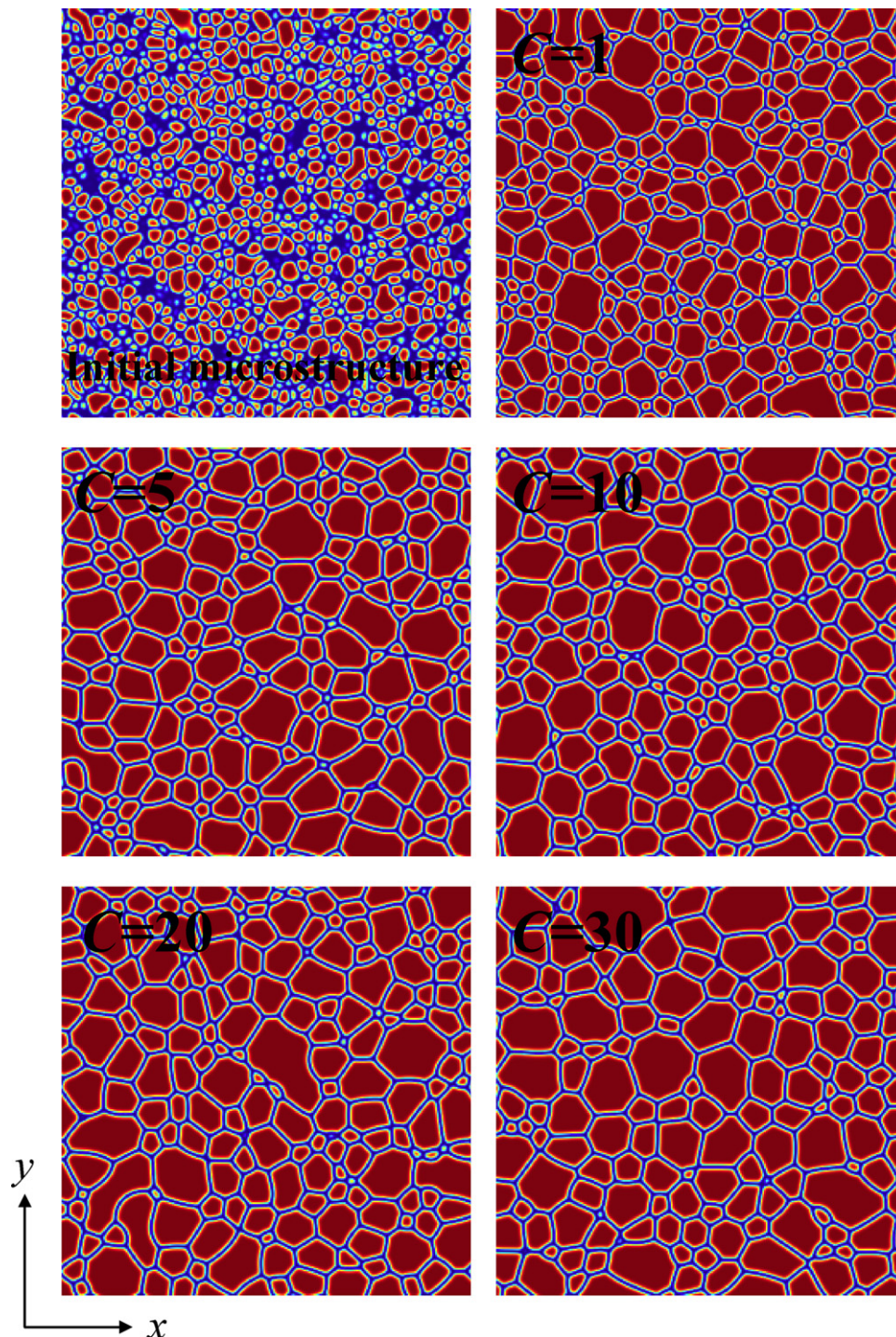


Fig. 6. Development of microstructures with different value of C viewed in x - y plane at $TS = 1.5$.

penetrate the grains with high mobility along the grain boundary until they form the equilibrium trijunction.

3.2. The average grain size

To analyze the microstructural changes quantitatively (Fig. 4), the average grain area was calculated and shown in Fig. 5. The average grain area is a function of time for simulation experiments. It can be noted that the average size of the equi-axial shape grains is seen to be bigger than the plate-like morphology grains. It should be attributed to that there are more grain boundaries and the relative mobility difference of the grain boundaries at the same direction is smaller as the microstructure evolves for the case of $C > 1$. The growth of the mean grain area is usually approximated by a simple power law:

$$\langle A \rangle^n - \langle A_0 \rangle^n = \alpha t. \quad (10)$$

where $\langle A \rangle$ denotes the average grain area at time t and $\langle A_0 \rangle$ is the initial grain area, n is the grain growth exponent. The simulation results shown in Fig. 5 are in agreement with the classical theories of grain growth. $n = 1$ (linear growth) is obtained for isotropic case ($C = 1$). When interface energy is anisotropic ($C > 1$), the growth is no longer linear and the value of n is less than 1. When $C > 10$, the growth behavior is similar to the one observed in the case of $C = 10$, which is in qualitative agreement with previous theoretical analytical (Eq. (8) and Fig. 2). The growth exponent of the case of $C > 1$ is smaller than the one obtained in the case with $C = 1$. The reason is that the anisotropic grain growth is prevented due to fast impingement of anisotropic grains, grain boundaries tend to be faceted. At the nucleation stage an increase in the value of C increased the velocity of the anisotropic grain growth. The time of impingement of anisotropic grains with the larger value of C is much shorter. Therefore, an increase in the value of C decreased the growth exponent and grain size in the x – z plane, which is different situation for x – y plane. In order to saving simulation time, the microstructure development in x – y plane

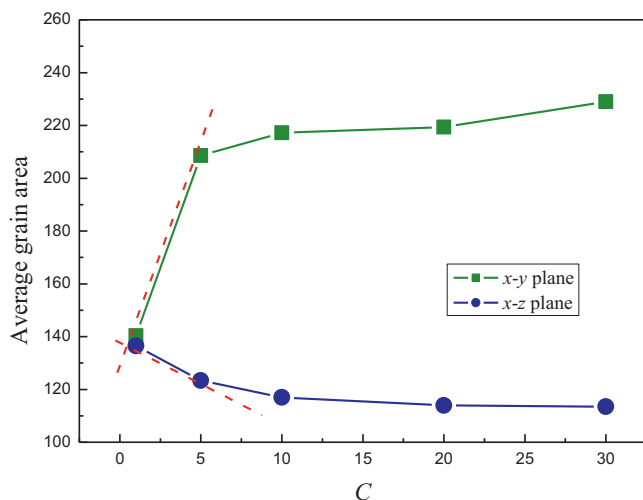


Fig. 7. Change of the average grain area in different 2D plane with C .

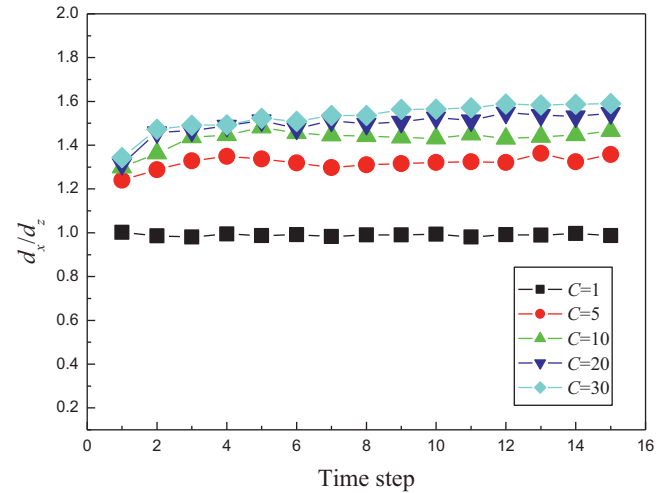


Fig. 8. Change in the value of d_x/d_z with time as a function of C .

was simulated in 256×256 grid points system as shown in Fig. 6. It can easily be seen that grain size increased with the increasing of the C value. However, the varied degree of the ratio between grain growth rates is larger in x – y plane than that of the case in x – z plane because of interface energy isotropy and anisotropy, as shown in Fig. 7. Obviously, grain growth rate is faster for the case of $C \geq 1$ in three dimensional space system.

3.3. Aspect ratio evolution

As has been illustrated qualitatively in Fig. 4, interface energy anisotropy could have a strong effect on grain shapes. To analyze this effect quantitatively, we calculate the average mean linear intercept (MLI) in the different directions (x -axis and z -axis) and compare their growth rates. The MLI, d_x and d_z , are in the horizontal, ' z ', and vertical, ' x ', directions, respectively. We calculate the MLI by following equations:

$$d_z = \sum_{i=1}^{512} \frac{1}{l_i} \quad (11)$$

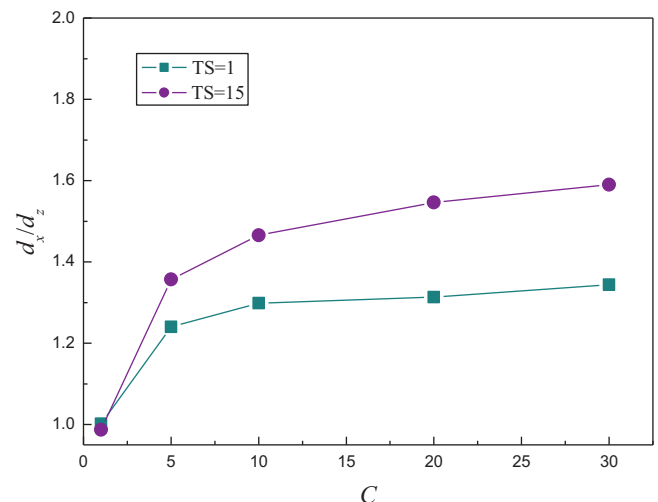


Fig. 9. d_x/d_z as a function of C .

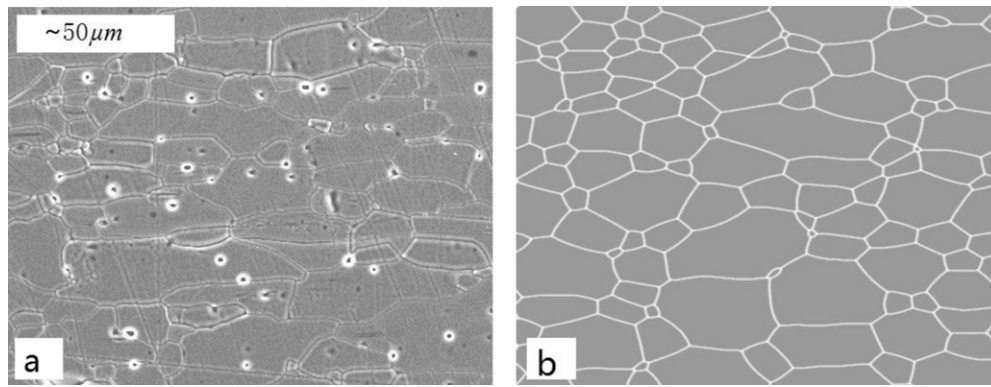


Fig. 10. The comparison of experimental data with simulation results: (a) SEM micrographs of textured SBN ceramics [19]; (b) simulation result at TS = 36.

where l_i is the number of grains i -line along z -axis crossed. The value of d_x can be obtained in the same way with d_z . Fig. 8 shows the ratio of d_x to d_z as a function of time. The ratio in an isotropic system ($C = 1$) is time-invariant and equal to unity, indicating that there is no preferred orientation in the system. However, when the interface energy is anisotropic ($C > 1$), the value of d_x/d_z is time-dependent and self-similarity does not hold anymore. The stronger anisotropic grains will be produced with the larger the value of C .

It is easily to note that grains in the system with anisotropic interface energy continue to slowly change their shapes throughout the entire simulation. It can be understood in the following manner. In the initial stage, the grains are small, have a large curvature and grain growth is mainly due to the decrease of the grain curvature. As the grains grow, the grain boundaries become less curved; but the anisotropy in interface energy allows the higher energy boundary to move faster than the lower energy boundary, so that the fraction of low boundaries increases. The grains become horizontally elongated. An increase in grain anisotropy is evident affected by the value of C . For the discussions below, we compare the results obtained at TS = 1 and 15. As shown in Fig. 9, an increase in the value of C increased the ratio of d_x to d_z . When the value of C is greater than 10, the ratio of d_x to d_z becomes a constant.

In order to comparison of simulation results with experimental data, the system of simulation was divided into 512×400 grid points. Due to the larger average grain size, we selected the value of C for 10 in simulations. The experimental data came from the textured $\text{Sr}_{0.5}\text{Ba}_{0.5}\text{Nb}_2\text{O}_6$ (SBN) ceramics fabricated by Zhao using RTGG technique [19]. Fig. 10(a) shows SEM photograph of textured SBN ceramics sintered at 1320°C . The size of SEM photograph is 512×400 pixels and the value of d_x/d_z is 1.71. Fig. 10(b) shows the simulation result at TS = 36. The value of d_x/d_z is 1.7066. The shape of grains in simulation is consistent with the experimental result obtained for textured SBN ceramics prepared by reaction templated grain growth.

4. Conclusions

The phase field model has been extended to take into account the grain-oriented growth. It was found that interface

energy anisotropy does significant change grain shapes from the one observed in isotropic system. The grain evolves in plate-like morphology rather than equi-axial shapes and the growth is no longer linear. The different value of anisotropic coefficient C does have an influence on the variation of grain anisotropy. An increase in the value of C increased the grain anisotropy with time. The simulation results are in agreement with qualitatively corresponding to the experimental results. This model can be easily used to simulation of grain-oriented microstructure of functional ceramics prepared by reaction templated grain growth.

Acknowledgments

This work was supported by Aviation Science Foundation of China, Basic Research Foundation of Northwestern Polytechnical University, and the Doctorate Foundation of Northwestern Polytechnical University (cx201010).

References

- [1] W. Yang, L.Q. Chen, G.L. Messing, Computer simulation of anisotropic grain growth, *Materials Science and Engineering A* 195 (1995) 179.
- [2] F. Gao, X.C. Liu, C.S. Zhang, Fabrication and electrical properties of textured $(\text{Na,K})_{0.5}\text{Bi}_{0.5}\text{TiO}_3$ ceramics by reactive-templated grain growth, *Ceramics International* 34 (2008) 403.
- [3] G.L. Messing, S. Trolier-McKinstry, E.M. Sabolsky, C. Duran, Templated grain growth of textured piezoelectric ceramics, *Critical Reviews in Solid State and Materials Sciences* 29 (2004) 45.
- [4] M.M. Seabaugh, I.H. Kerscht, G.L. Messing, texture development by templated grain growth in liquid-phase-sintered α -alumina, *Journal of the American Ceramic Society* 80 (5) (1997) 1181.
- [5] F. Gao, R.Z. Hong, J.J. Liu, Effect of different templates on microstructure of textured $\text{Na}_{0.5}\text{Bi}_{0.5}\text{TiO}_3$ – BaTiO_3 ceramics with RTGG method, *Journal of the European Ceramic Society* 28 (10) (2008) 2063.
- [6] N. Louat, On the theory of normal grain growth, *Acta Metallurgica* 22 (1974) 721.
- [7] A. Kuprat, D. George, G. Straub, Modeling microstructure evolution in three dimensions with Grain3D and LaGriT, *Computation Materials Science* 28 (2003) 199.
- [8] E. Fjeldberg, K. Marthinsen, Computational design for grain-oriented microstructure of functional ceramics prepared by templated grain growth, *Computation Materials Science* 48 (2010) 267.
- [9] J. Geiger, A. Roosz, P. Barkoczy, Simulation of grain coarsening in two dimensions by cellular-automaton, *Acta Materialia* 49 (2001) 623.

- [10] N. Moelans, B. Blanpain, P. Wollants, An introduction to phase-field modeling of microstructure evolution, *Calphad—Computer Coupling of Phase Diagrams and Thermochemistry* 32 (2008) 268.
- [11] L. Vanherpe, N. Moelans, B. Blanpain, S. Vandewalle, Phase-field models for microstructural evolution, *Computation Materials Science* 49 (2010) 340.
- [12] S. Vedantam, A. Mallick, Phase-field theory of grain growth in the presence of mobile second-phase particles, *Acta Materialia* 58 (2010) 272.
- [13] L.M. McKenna, M.P. Gururajan, P.W. Voorhees, Phase field modeling of grain growth: effect of boundary thickness, triple junctions, misorientation, and anisotropy, *Journal of Materials Science* 44 (2009) 2206.
- [14] N. Moelans, B. Blanpain, P. Wollants, Quantitative phase-field approach for simulating grain growth in anisotropic systems with arbitrary inclination and misorientation dependence, *Physical Review Letters* 101 (2008) 025502.
- [15] N. Moelans, B. Blanpain, P. Wollants, Quantitative analysis of grain boundary properties in a generalized phase field model for grain growth in anisotropic systems, *Physical Review B* 78 (2008) 024113.
- [16] A. Kazaryan, Y. Wang, S.A. Dregia, B.R. Patton, Grain growth in anisotropic systems: comparison of effects of energy and mobility, *Acta Materialia* 50 (2002) 2491–2502.
- [17] L.Q. Chen, Phase-field models for microstructure evolution, *Annual Review of Materials Science* 32 (2002) 113–140.
- [18] L.Q. Chen, W. Yang, Computer simulation of the domain dynamics of a quenched system with a large number of nonconserved order parameters: the grain-growth kinetics, *Physical Review B* 50 (1994) 15752–15756.
- [19] L.L. Zhao, Preparation and electric properties of strontium barium niobate-based lead-free piezoelectric textured ceramics, Ph.D. Thesis, Northwestern Polytechnical University, 2005.